XXV CONGRESO DE ECUACIONES DIFERENCIALES Y APLICACIONES
XV CONGRESO DE MATEMÁTICA APLICADA
DEL 26 AL 30 DE JUNIO DE 2017
CEDYA+CMA
XXV CONGRESO DE ECUACIONES DIFERENCIALES Y APLICACIONES
XV CONGRESO DE MATEMÁTICA APLICADA
CARTAGENA - 2017

GIS-integrated environmental models

M.I. Asensio*, D. Prieto*, D. Álvarez*, L. Ferragut* and J.M. Cascón†

Abstract— In this paper, we present the integration of the mathematical models *Physical Forest Fire Spread* (PhFFS) and *High Definition Wind Model* (HDWF), developed by the authors, into a GIS-based interface in order to supply to the end-user a functional and efficient tool. The resulting tool automates data acquisition, pre-processes spatial data, launches the aforementioned models, and displays the corresponding results in a unique environment. Our implementation uses the Python language and Esri's ArcPy library to extend the functionality of ArcMap 10.4. The PhFFS is a simplified 2D physical wildland fire spread model based on conservation equations, with convection and radiation as heat transfer mechanisms. It also includes some 3D effects. The HDWF arises from an asymptotic approximation of the Navier-Stokes equations, and provides a 3D wind velocity field in an air layer above the terrain surface. Both models can be run in standalone or coupled mode. Finally, we confirm that the developed tool is efficient and fully operational presenting some examples of its successful application.

1 Introduction

Mathematical models can be useful in decision-making processes, particularly in complex environmental decision problems. Moreover, these models provide truly interesting mathematical and computational problems. But the final goal is to supply to the end-user a functional and efficient tool. This implies the need for interdisciplinary collaboration, and the use of spatial data management tools as Geographic Information Systems (GIS).

Wildland fires have become one of the most pressing environmental, social and economic issues threatening the world forests. According to the latest annual report issued by European Forest Fire Information System [25], Spain and Portugal are the European countries most affected by wildfires. The threat of wildland fires is increasing due to global warming [15], so there is considerable interest in minimising the risk and mitigating the damage they cause. Therefore, the real-time simulation of wildland fire spread has direct applications in prevention (risk mapping, reforestation policies, and the design of fuelbreaks), in fire-fighting (predicting a fire's pathway helps to mobilise and optimise resources, improve firefighters safety during extinguishing works, issue warnings, and evacuation planning), and in prescribed burn planning.

Furthermore, one of the factors most influencing wildfire spread is the wind [26]. Topographically modified wind fields and coupled fire and transport models are necessary to properly describe wildfire behaviour [18]. Wind models have other specific applications, such as wind power forecasting on wind farms.

Two different models have been developed by the authors: a Physical Forest Fire Spread model (PhFFS) and a High Definition Wind field Model (HDWF). The PhFFS model is a simplified 2D semi-physical wildland fire spread model based on conservation equations, with convection and radiation as main heat

*Departamento de Matemática Aplicada, Universidad de Salamanca, Casas del Parque 2, 37008–Salamanca(SPAIN). Email: mas@usal.es, dprieto@usal.es, dalle@usal.es, ferragut@usal.es

†Departamento de Economía e Historia Económica, Universidad de Salamanca, Edificio FES, Campus Miguel de Unamuno, 37007–Salamanca(SPAIN). Email: casbar@usal.es

transfer mechanisms, that includes some 3D effects and takes into account topography, wind, fuel moisture content and fuel type. The numerical solution of the model equations involves efficient numerical and computational tools for simulating real fire events in less than real time [10, 8, 9]. The HDWF lies in an asymptotic approximation of the primitive Navier-Stokes equations, with the aim to provide a 3D velocity wind field, solving only 2D linear equations [5]. Solving an optimal control problem in which the wind flow on the surface boundary is the control, the model provides a 3D wind field adjusted to several meteorological wind data at some points of the domain [12].

In order to bring these models to the end-user through a readily accessible, intuitive and easy-to-use tool, a GIS-based interface has been developed integrating both models. The development of this tool is based on the extent of the functionality of the commercial software ArcGIS Desktop, through the Python scripting language and the Esri ArcPy library. This tool also facilitates the testing and validation process of the models, by automating and simplifying the spatial data acquisition procedure and the display of the solution.

2 The models

In this section we briefly describes the underpinnings of the two models coupled with the GIS to provide the operational wildland fire simulation GIS-based tool: PhFFS and HDWF. We also outline both models input and output variables and parameters as a step towards their integration into a GIS.

2.1 PhFFS

The Physical Forest Fire Spread (PhFFS) is the current version in a series of physical fire propagation models developed by the authors. It has its origin in a simple 2D one-phase physical model, based on the principles of energy and mass conservation, and considers convection and diffusion. Heat transfer by radiation was incorporated into the model with a local radiation term in [3]. The influences of fuel moisture content and heat absorption by pyrolysis were included in [11] with an operator representing enthalpy. At the same time, the non-local radiation from the flames above the vegetal layer was added to the model in [10], enabling it to deal with the effect that wind and slope had over flame tilt, giving rise the current PhFFS model. Further efforts have been made to improve the suitability of the PhFFS model for the simulation of real fires in [8] and experimental fires in [24], with the introduction of data assimilation techniques in [9].

The dimensionless simplified equations of the PhFFS model,

$$\partial_t e + \beta \mathbf{v} \cdot \nabla e + \alpha u = r \quad \text{in } S \times (0, t_{max}), \tag{1}$$

$$e \in G(u) \quad \text{in } S \times (0, t_{max}), \tag{2}$$

$$\partial_t c = -g(u)c \quad \text{in } S \times (0, t_{max}). \tag{3}$$

are completed with homogeneous Dirichlet boundary conditions and the following initial conditions,

$$u(x, y, 0) = u_0(x, y) \quad \text{in } S, \tag{4}$$

$$c(x, y, 0) = c_0(x, y) \quad \text{in } S. \tag{5}$$

The spatial domain S represents the surface where the fire occurs, defined by the mapping,

$$\begin{array}{ll} S: d & \longmapsto \mathbb{R}^3 \\ (x, y) & \longmapsto (x, y, h(x, y)) \end{array}$$

where $h(x, y)$ is a known function representing the topography of the surface S and $d = [0, l_x] \times [0, l_y] \subset \mathbb{R}^2$ is a rectangle representing the projection of the surface S.

The unknowns, $e = \frac{E}{MCT_\infty}$, dimensionless *enthalpy*, $u = \frac{T - T_\infty}{T_\infty}$, dimensionless *temperature of the solid fuel* and $c = \frac{M}{M_0}$, dimensionless *mass fraction of solid fuel*, are bidimensional variables defined in $S \times (0, t_{max})$, where t_{max} is the time of study. All the physical quantities referred here and their units are listed in Table (1).

The model takes into account the energy lost by natural vertical convection through the term αu in the energy conservation equation (1). This term is related to the *natural convection coefficient* $\alpha = \frac{H[t]}{MC}$, where H $(J\, s^{-1}\, m^{-2}\, K^{-1})$ is one of the three model parameters, representing the natural convection, and $[t]$ is a time scale.

The expression $e \in G(u)$ (2) represents a multivalued operator that models the influence of solid fuel moisture content,

$$G(u) = \begin{cases} u & if \quad u < u_v, \\ [u_v\ ,\ u_v + \lambda_v] & if \quad u = u_v, \\ u + \lambda_v & if \quad u_v < u < u_p, \\ [u_p + \lambda_v\ ,\ \infty] & if \quad u = u_p, \end{cases}$$

and depends on dimensionless *pyrolysis temperature* u_p, dimensionless *evaporation temperature of the water* u_v and on dimensionless *evaporation heat* $\lambda_v = \frac{M_v \Lambda_v}{CT_\infty}$, related to the latent heat of evaporation Λ_v $(J\, kg^{-1})$ and the fuel moisture content M_v (kg of water/kg of dry fuel). For further details about this multivalued operators see [11]. It is should mentioned that both, pyrolysis temperature and fuel moisture content, are related to fuel type.

The PhFFS model considers wind effect in two different ways: through the convective term itself and through the flame tilt caused by wind that affects the radiation term. The convective term, $\beta \mathbf{v} \cdot \nabla e$ in energy conservation equation (1), represents the energy convected by the gas pyrolyzed through the elementary control volume, where the *surface wind velocity*, $\mathbf{v}$, is rescaled by a *correction factor* β. For a detailed explanation of this second model parameter β see [9]. The surface wind velocity $\mathbf{v}$ can be collected from meteorological stations located close to the fire; these wind velocity data can be considered as

constant wind data or can be used to adjust a wind field over the simulation area by a wind model as the HDWF described bellow.

The right hand side of equation (3) represents the loss of solid fuel due to combustion,

$$g(u) = \begin{cases} 0 & if \quad u < u_p, \\ \gamma & if \quad u = u_p, \end{cases}$$

i.e., the loss of solid fuel is null if the temperature is below the pyrolysis temperature, and it remains constant when the temperature of pyrolysis is reached. This constant value is inversely proportional to the solid fuel half-life time $t_{1/2}$ of the combustion of each type of fuel,

$$\gamma = \frac{\ln 2[t]}{t_{1/2}}.$$

The right hand side of the energy conservation equation (1) describes the thermal radiation reaching the surface S from the flame above the layer.

$$r = \frac{[t]}{MCT_\infty} R.$$

R represents the incident energy at a point $\mathbf{x} = (x, y, h(x, y))$ of the surface S due to radiation from the flame above the surface per unit time and per unit area, obtained by summing up the contribution of all directions $\mathbf{\Omega}$; that is

$$R(\mathbf{x}) = \int_{\omega=0}^{2\pi} I(\mathbf{x}, \mathbf{\Omega}) \mathbf{\Omega} \cdot \mathbf{N} \, d\omega, \tag{6}$$

where ω is the solid angle and $\mathbf{N}$ is the unit outer vector normal to the surface S, considering only the hemisphere above the surface point. Each contribution depends on the flame length F, and I is the total radiation intensity.

The differential equation describing the total radiation intensity I at any position along a given path s in a gray medium may be written neglecting scattering as

$$\frac{dI}{ds} + a(s)I(s) = a(s)I_b(s), \tag{7}$$

where I_b is the black body total radiation intensity and is governed by the Stefan-Boltzmann law, corresponding to the integral over all wavelengths of the emissive power of a black body

$$I_b = \frac{\sigma}{\pi} T^4, \tag{8}$$

where $\sigma = 5.6704 \times 10^{-8} Js^{-1}m^{-2}K^{-4}$ is the Stefan-Boltzmann constant and the temperature T reaches the flame temperature denoted by T_f. Both, flame length F and flame temperature T_f, depend on fuel type. a is the radiation absorption coefficient inside the flame and is the third model parameter. For further details about the radiation computation see [9].

After this brief explanation of the PhFFS model equations, in order to understand how the interface between the GIS and the model has been developed, we should point out the different elements in the model equations (Table 1). The equation unknowns (model magnitudes), mainly the solid fuel mass fraction c and the non-dimensional solid fuel temperature u, define the initial input state, and the output variables to be displayed. All other input variables define each simulation scenario, and can be fuel type dependent or not (see Table 1). Finally, we should distinguish the model parameters, unknown values that should be adjusted, although their physical meaning can provide an approximate idea of their ranges.

Table 1: Equation unknowns (dimensionless unknowns), input variables (no fuel type and fuel type dependent) and parameters for PhFFS.

Unknown	Symbol	Units
Enthalpy	$E\ (e)$	$J\,m^{-2}$
Solid fuel temperature	$T\ (u)$	K
Fuel load	$M\ (c)$	$kg\,m^{-2}$
Input variable	**Symbol**	**Units**
Wind velocity	$\mathbf{v}$	$m\,s^{-1}$
Reference temperature	T_∞	K
Surface height	h	m
Latent evaporation heat	Λ_v	$J\,kg^{-1}$
Input variable (fuel type)	**Symbol**	**Units**
Maximum fuel load	M_0	$kg\,m^{-2}$
Moisture content	M_v	kg water$/kg$ fuel
Flame temperature	T_f	K
Pyrolysis temperature	T_p	K
Combustion half-life	$t_{1/2}$	s
Flame length	F	m
Heat capacity	C	$J\,K^{-1}\,kg^{-1}$
Parameter	**Symbol**	**Units**
Mean absorption coeff.	a	m^{-1}
Natural convection coeff.	H	$J\,s^{-1}\,m^{-2}\,K^{-1}$
Convective term factor	β	$-$

The numerical solution of equations (1,2,3) is based on $P1$ finite element approximation on a regular mesh for spatial discretization and a Crank-Nicolson finite difference scheme for time discretization of the total derivative (characteristic method for the convective term) combined with an Euler half-step for the radiation term. For each time step, the corresponding discretised expressions for temperature, enthalpy and fuel load can be computed separately for each spatial node, so their calculation can be paralellized. The radiation term (6) is computed with an exact integration method assuming a rectangular flame shape (under windy conditions we assume tilted flames) for the non-local radiation equation, through an analytical expression of the solution of the intensity ordinary differential equation (7) in terms of the optical thickness [9]. In order to reduce the computational time, the equations are only figured out using the *active nodes* placed around the perimeter

where the fire occurs, since the operations only affects to the involved nodes in the fire front and not to all nodes in the domain. These efficient numerical methods, together with different parallel computing techniques, ensure that the computational cost of running the PhFFS model has been significantly reduced, whereby it can compete with other simpler models and allows to sustain the computational cost of data assimilation techniques. For a detailed explanation on different aspect of the numerical solution of the PhFFS model see [8] and [9].The PhFFS model is implemented in C++, using API OpenMP [6] in order to exploit multiprocessor platforms for reducing computational time.

One of the most difficult development challenges of the PhFFS model is its accurate adjustment. Some of its input variables are difficult to measure, this combined with the uncertainty of its parameters, makes the model adjustment a highly complex process. Faced with this situation, a sensitivity analysis of the models is an important previous step towards an efficient parameter adjustment design, as this identifies the most influential factors (input variables and parameters). [24] have conducted a global sensitivity analysis of the PhFFS model, concluding that the model properly reflects the importance of radiation in no-wind conditions, and convection in windy conditions. In addition, the fire model parameters have been adjusted to show that their values remain within the same order of magnitude, independently of the different conditions given by the input variables. The integration of PhFFS into a GIS platform will facilitate the model adjustment process.

2.2 HDWF

The first results that gave rise to the High Definition Wind-Field model HDWF was published in [4], where the coupling of both, wind and fire model, has already arisen. The idea behind this convection model is an alternative to the classical shallow water models. In both cases the horizontal dimensions are much larger than the vertical one, but the HDWF provides a three-dimensional velocity wind field in the air layer under the influence of the fire, governed by solving only two-dimensional linear equations, so that it can be coupled with the two-dimensional fire spread model. This wind model was initially developed for the first fire model with local radiation. The details of how an asymptotic approximation of the primitive Navier–Stokes equations can be derived are set out in [5]. More precisely, the described model computes explicitly the three-dimensional air velocity as a function of the vertical coordinate, a stream function, the surface temperature, the surface height and the meteorological wind flow on the surface boundary. The model depends on a single parameter, the air friction coefficient which is related with the roughness length of the surface. The validity of this wind model has the following limits: the nonlinear terms are neglected and it is assumed that the temperature linearly decreases with the height. Nevertheless, the model takes into account buoyancy forces, slope effects and mass conservation.

In [12] the wind field obtained by the model is adjusted to several punctual wind velocity measurements at different points in the three-dimensional domain by an optimal control problem in which the wind flow on the surface boundary is the control. The optimal control problem is solved using the adjoint equation-based method. In this way using the meteorological wind punctual measures as datum, the HDWF model provides locally a detailed three-dimensional wind field in an air layer over a surface, taking into account topography and thermal gradients on the surface by solving only two-dimensional linear equations. This is how the HDWF model is used together with the PhFFS model with non-local radiation, since it must be taken into account the effect of wind (and also slope) on the flame tilt in order to compute the radiation. Moreover, the coupled use of both models, HDWF and PhFFS models, would allow to take into account the influence of thermal effects, such as the high temperatures that occur during a fire, on the wind.

In [13] this model was compared with a three-dimensional mass consistent wind model and it is applied to a realistic example estimating the main parameters of the model by using genetic algorithms and parallel computations.

The three-dimensional domain is

$$D=\{(x,y,z)\colon (x,y)\in d, h(x,y)< z< \delta\},$$

where δ represents the thickness of the air layer that is small compared with its width, but covers the air layer under the influence of a fire temperature. This is necessary in order to consider the effect of wildland fires temperatures into the simulated wind field. The ground surface S is the lower boundary of D, and $A=\{(x,y,z) : (x,y)\in d,\ z=\delta\}$ is the air upper boundary of D.

Using the fact that the 3D domain is a thin layer and assuming that the surface is not too rough, the asymptotic wind equations in D are,

$$-\partial^2_{zz}\mathbf{V}+\boldsymbol{\nabla}_{xy}P = 0, \tag{9}$$

$$\partial_z P = \lambda\tilde{T}, \tag{10}$$

$$\boldsymbol{\nabla}_{xy}\cdot\mathbf{V}+\partial_z W = 0, \tag{11}$$

where $\mathbf{V}=(V_1,V_2)$ are the horizontal components of the 3D wind, W is the vertical component, P is the pressure, $\tilde{T}$ is the temperature and λ is related to the Grashof number. It should be noted that all this variables are defined on the 3D domain, particularly $\tilde{T}$ is the 3D temperature, while T is the 2D temperature on the surface S.

The boundary conditions of the asymptotic model are,

$$\partial_z\mathbf{V}=\zeta\mathbf{V},\quad (\mathbf{V},W)\cdot\mathbf{N}=0,\quad \text{on } S, \tag{12}$$

$$\partial_z\mathbf{V}=0,\quad W=0,\quad \text{on } A, \tag{13}$$

$$\overline{\mathbf{V}}\cdot\boldsymbol{\eta}=(\overline{\delta}-h)\mathbf{v}_m\cdot\boldsymbol{\eta},\quad \text{on } \partial d, \tag{14}$$

where $\mathbf{N}$ is the inner unit normal vector field to ∂D, $\boldsymbol{\eta}$ is the inner unit normal vector field to ∂d, ζ is the friction coefficient,

$\mathbf{v}_m$ is the horizontal component of the meteorological wind, not depending on z and with a null total flux through the lateral boundary. $\overline{\mathbf{V}}$ is the horizontal flux at a point $(x, y) \in d$ and time t, and is defined by

$$\overline{\mathbf{V}}(x,y) = \int_{h(x,y)}^{\delta} \mathbf{V}(x,y,z)\, dz. \tag{15}$$

If we assume that the air temperature decreases linearly with height and vanishes on the upper boundary, by analytical integration of equation (10) the asymptotic problem can be reduced to solve the following bidimensional problem

$$-\boldsymbol{\nabla}_{xy} \cdot (a\boldsymbol{\nabla}_{xy} p) = \boldsymbol{\nabla}_{xy} \cdot (b\boldsymbol{\nabla}_{xy} T_S) \quad \text{in } d, \tag{16}$$

$$a\boldsymbol{\nabla}_{xy} p \cdot \boldsymbol{\eta} = -b\boldsymbol{\nabla}_{xy} T_S \cdot \boldsymbol{\eta} + v \quad \text{on } \partial d, \tag{17}$$

where the potential p depends only on the two first spatial variables (x, y); T_S is a rescaled 2D temperature depending on ground surface temperature T and

$$v = v(x,y) = (\overline{\delta} - h(x,y))\mathbf{v}_m(x,y) \cdot \boldsymbol{\eta}$$

is the horizontal flux on ∂d.

Thus, the horizontal wind is given by,

$$\begin{aligned} \mathbf{V}(x,y,z) = m(x,y,z)\boldsymbol{\nabla}_{xy} p(x,y) + \\ +n(x,y,z)\boldsymbol{\nabla}_{xy} T_S(x,y), \end{aligned} \tag{18}$$

and $\mathbf{v}(x, y) = \mathbf{V}(x, y, 0)$ is the value used in the convective term of the fire model in equation (1).

Functions a, b, m and n depend on $\overline{\delta}$, h and the inverse of the friction coefficient.

Table 2: Magnitudes, input variables and parameters for HDWF.

Unknown	Symbol	Units
Wind velocity	$\mathbf{V}$	$m\,s^{-1}$
Potential	p	s^{-1}
Input variable	**Symbol**	**Units**
Horizontal component meteo. wind	$\mathbf{v}_m$	$m\,s^{-1}$
Surface air temperature	T	K
Height of the surface	h	m
Roughness length	z_0	m
Parameter	**Symbol**	**Units**
Friction coefficient	ζ	$-$

This model requires knowledge of the horizontal wind flux v through ∂d, which is currently unknown. Usually, the meteorological wind at a finite number of points over the surface S is known. In [12] we propose a way to solve the bidimensional potential problem given by equations (16) and (17) as an optimal control problem: given n experimental measurements of the wind velocity $\mathbf{V}_i,\ i = 1, \ldots, n$, at n given points $P_i = (x_i, y_i, z_i)$, $i = 1 \ldots n$, we search for the value of v, the solution of equations (16) and (17), such that the $\mathbf{V}(x_i, y_i, z_i)$ given by equation (18) are as close as possible to the experimental values $\mathbf{V}_i$.

For more details of how the equations of this wind model are derived and about the optimal control problem see [5, 12].

3 GIS-integration

The integration of the PhFFS and HDWF models into a GIS tool achieves several objectives. First of all, it provides a simple, intuitive and easy-to-use tool that is more accessible to a broader audience that might not be familiar with these models. Furthermore, the automation of the data acquisition and processing of all the geographical information required simplifies the simulation process reducing simulation time. It also prevents input data errors by the standardization of the georeferenced input data.

This section describes all the work performed to implement a GIS integrated tool for both models, PhFFS and HDWF. Two different developments must be distinguished: the geodatabase and the GIS interface.

3.1 Geodatabase development

It should be note that the tool is initially developed for its use throughout Spain, so the scope of the geographic data used is limited to Spain. It is important to stress that most of the spatial data analysis and assembling operations have been automated through several scripts with the objective to simplify the work required to extend the use of the developed tool to other areas.

Focusing on Spain, we define a common spatial reference for all the heterogeneous spatial data resources. According to Spanish regulations, the selected spatial reference is the Projected Coordinate System *ETRS1989 UTM Zone 30N*, except for the Canary Islands, where the Projected Coordinate System *ETRS1989 UTM Zone 28N* is used instead.

Three different maps have been compiled: an *elevation map*, and a *fuel type distribution map*, both required by the PhFFS model and the HDWF; and a third map to locate all the elements involving the function of either artificial or natural firebreaks that affect the fire spread (barren land, water bodies, transport infrastructures, etc.) required only by the PhFFS model, that we denote *fuel load map*. This previous map production allows to automate and simplify the spatial data acquisition reducing simulation time and providing a robust and reliable system that prevents data entry error. This former work also enables to reduce the simulation time since the pre-process work during the simulation is limited to clip the necessary data corresponding to the simulation area.

The elevation map is a raster type file generated from the digital terrain model MDT05 with 5-meter spatial resolution from

the Spanish National Geographic Institute [17]. The more than 1.000 initial files were projected in the corresponding coordinate system and merged into two integer type raster corresponding to mainland Spain and Balearic Islands (13GB), and Canary Islands (356MB).

The fuel type distribution map is a shapefile generated from the *Spanish Forestry Map* 1:25.000 (MFE25) [23] combined with the *Fourth Spanish National Forest Inventory* (IFN4) [21] or the *Spanish Forestry Map* 1:50.000 (MFE50) [19] with the information from the *Third Spanish National Forest Inventory* (IFN3) [20]. Both inventories have been developed by the *Ministry of Agriculture, Food and Environment* of the Spanish Government. The more recent IFN4 is not yet available for the whole of Spain. The inventory data corresponding to the BEHAVE fuel classification system [1] have been filtered and the corresponding shape files have been properly projected. In order to reduce the file size, a combining and smoothing process has been applied.

The fuel load map is a shapefile that supplies all the elements involving the function of either artificial or natural fuelbreaks that affect the fire spread. These data have been extracted from the *Spanish Land Cover Information System* (SIOSE) [16] by selecting all the surfaces where a fire can not occur (barren land, water bodies, transport infrastructures, etc.), providing zero load fuel data for the model. Work is currently under way to improve the fuel load map by incorporating the information from the *Spanish National Topographic Base Map* 1:25.000 (BTN25) [22]. This base map contains 760.000 files with 88 different data layers. All these data should be analysed and the necessary data for the PhFFS model should be collected, projected and processed.

3.2 GIS interface development

The PhFFS and HDWF models have an interface provided through ASCII grid text files as inputs and outputs. The GIS software is used to build these *ASCII grid text files* for each simulation scenario, calls the standalone executables of the models and reads their outputs in order to visualize them. This layout guarantees the same behaviour of the models both within or outside the GIS platform, reducing the amount of testing and validation required by the whole system.

The GIS tool chosen for the integration of our models, ArcMap 10.4 of Esri's ArcGIS Desktop suite, provides options for expanding its features through custom tools. The interface for the PhFFS and HDWF models has been developed as a *Python Add-in* for ArcMap [1]. The add-in developed includes a menu and a toolbar that contains a collection of custom tools designed to facilitate the use of the PhFFS and HDWF models. The functionality of each tool is implemented as a script using the Python programming language and the ArcPy geoprocessing library [7]. These scripts are run each time the user presses a button on the toolbar or on the menu, or fires a mouse event over the basemap.

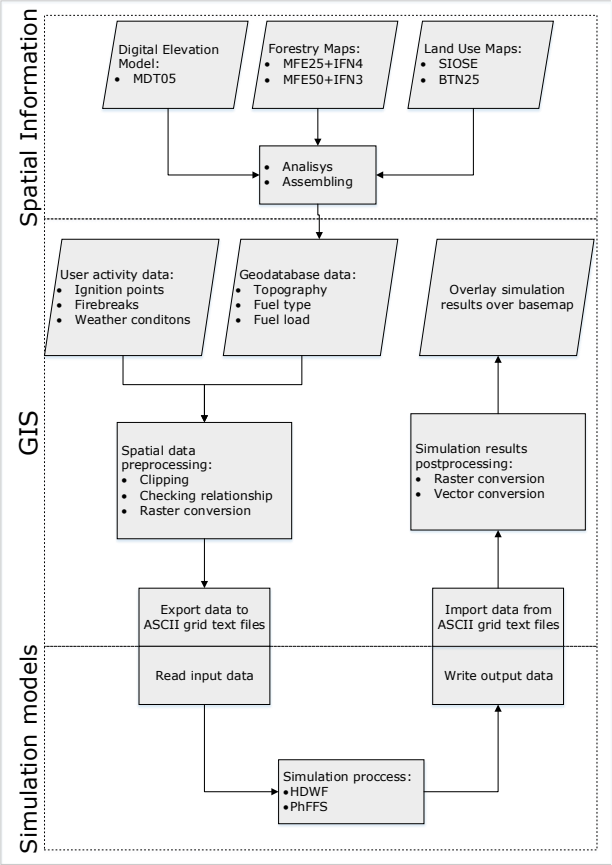

Figure 1: GIS-PhFFS-HDWF integration flow diagram.

Following the flow diagram in Figure 1, once we have loaded the basemap layer, we select the area of study and set the information over the basemap to simulate a specific scenario: ignition points, wind data, and eventually firebreaks, using the corresponding menu option or toolbar option or mouse event. The tool is designed to enables the user to eventually access and modify the numerical default values of models fuel type dependent input variables and parameters. This option is essential in order to assist in the complex models adjustment process. All this information and the corresponding spatial data for the selected area are pre-processed: clipped, checked to avoid errors, converted to raster, and exported to ASCII grid text files. The PhFFS and HDWF read the files they need, and the simulation is run providing the corresponding output ASCII grid text files. The post-processing step converts the output ASCII files to raster and vector files in order to display them over the basemap. All the raster and vector layers used during the same

[1] ArcGIS® and ArcMap™ are the intellectual property of Esri and are used herein under license. Copyright© Esri. All rights reserved. For more information about Esri® software, please visit www.esri.com.

simulation process are geo-referenced to the same geographical area, and have the same resolution and dimensions.

The PhFFS model provides two types of output data: the solid fuel mass fraction c and the non-dimensional solid fuel temperature u. Comparing the output solid fuel mass fraction with the initial fuel mass fraction inputted into the model provides the state of the landscape. So for each point of the domain we can determine whether or not that specific point has been burnt. This information is transformed to a vector layer and represented on the basemap in order to establish the *fire perimeter* at different instants, using a layer for each time step. The solid fuel temperature is also transformed into a vector layer and represented on the basemap for identifying those areas burning at the indicated time step, establishing the *fire front position* (see Figure 3).

Likewise, the wind velocity data that the HDWF provides at different layers over the ground surface can be displayed. We represent the resulting wind field by combining this information on a feature class, and we use its attributes (module and direction) for setting the corresponding colors and arrows with the right rotation. As ArcMap can only visualize 2D scenarios, we represent the wind data corresponding to each level by using a different layer for each height level (see Figure 2).

4 Real examples

We present here two examples of successful applications of the GIS integrated PhFFS model, as well as the use of the HDWF to simulate the wind field in the wildfire simulation process.

4.1 Osoño fire

The first example is the simulation of a real wildfire occurred near Osoño, Ourense province, in north-western Spain, one of the country's most fire-affected areas. The fire ignited at 3.45 p.m. local time, on 17 August 2009. The fire-fighting team had failed to stabilise the fire by 11.00 p.m. on the same day, but brought it under control at 3.45 a.m. on the following day, and finally extinguishing it at 9.10 p.m. on 18 August. The fire burned 224 ha: 185 ha of forest area (83 ha. were tree-covered interspersed with heath) and 39 ha. of agricultural area.

The initial burnt area was covered mainly with *Pinus pinaster*, the middle area was covered with dormant brush and to a lesser extent short grass and timber grass. The end burnt area was covered with diverse fuel types, mainly brush. Basin areas and property lines were covered by thick forest. The IFN4 data show some discrepancies with the observed data because the area where this fire occurred has been affected by several fires over the years, and these data are not regularly updated. This discrepancy between the available data and the actual data poses one of the challenges that fire simulation has to tackle.

The burnt area is located at an altitude ranging from 540 metres (ignition point area) to 680 metres (end fire area) above sea level. The average slope ranges from 6.56% at the beginning of the fire, to 2.86% at the end. For the first hours, the fire spread over an uneven surface, with positive and negative discontinuous slopes, with watersheds and river basins; for the final part, although the altitude is higher, the surface is relatively flat.

Weather data (wind, temperature and relative humidity) were collected every ten minutes at a nearby weather station (3750 m away) at a height of 10 m and were incorporated into the simulation process every 30 minutes. Figure 2 shows the wind field simulated with the HDWF at a height of 10 meters, corresponding to meteorological data at 7.00 p.m.

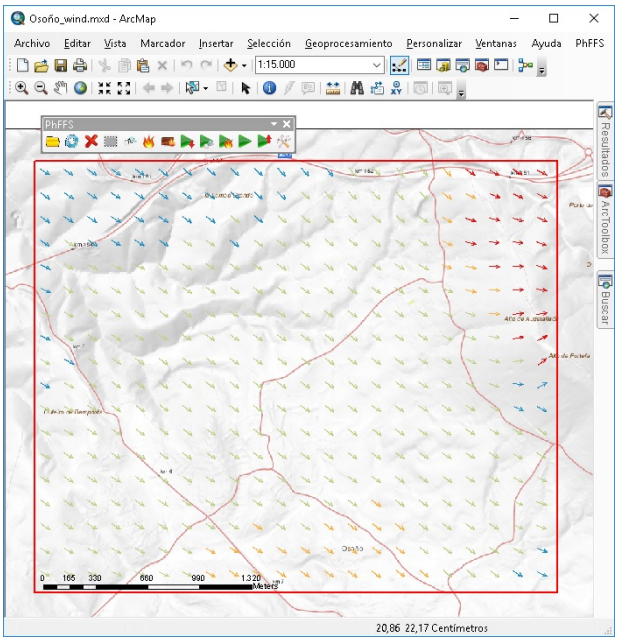

Figure 2: Screenshot of the GIS interface displaying the wind field simulated with HDWF at 7.00 p.m., at a height of 10 meters, along the simulation area for the Osoño fire.

The coupling effect of wind and topography considerably influenced this fire spread rate and direction. Initially, wind velocity was moderate, about $3.18\,m/s$ from the west. As the afternoon progressed the wind velocity increased to $4.79\,m/s$ with gusts of almost $8\,m/s$, and turning slightly to the north. This caused secondary fire sources due to the transport of firebrands by convection columns. Most of the fire-fighters' actions by land and air over the fire flanks are not reflected in the simulation, nor are the secondary fire sources, due to insufficient information, except those firebreaks made by widening some existing roads, where the available information is sufficiently detailed. Despite that and the discrepancies between the available fuel data and the real fuel data, the simulated and actual perimeters are quite similar, as shown in Figure 3. Some similarity indexes [14] have been calculated, obtaining average values that show substantial agreement (index≥ 0.6) between

the actual and simulated perimeters: Sørensen similarity index $S = 0.74$, Jaccard similarity coefficient $J = 0.59$ and Kappa coefficient $K = 0.71$.

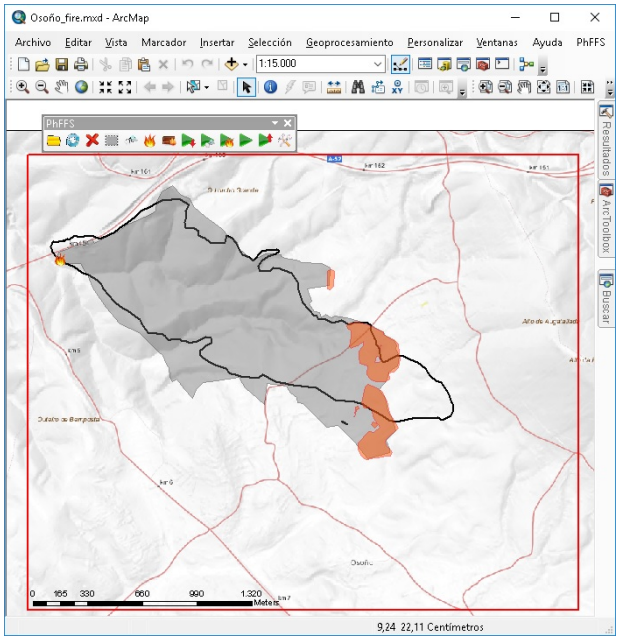

Figure 3: Comparison of the actual perimeter (black line) and simulated fire after four hours in Osoño fire, Ourense, 17 August 2009. Grey area shown the simulated burnt area, orange indicates the active fire front.

In this example, the simulation area is a rectangle of $3.315\,m \times 2.740\,m$, and the simulation of each hour of fire spread involves about 4.30 minutes of computational time on a laptop equipped with an Intel i5-2410M processor (two cores, each one working at a frequency of 2.30 GHz) and 8 GB RAM. A total of 4 hours and a half have been simulated, updating wind data every half hour, with a total simulation time of 20 minutes.

4.2 Cardona fire

The second example is the simulation of larger wildfire that took place in Catalonia on 8th July 2005 that burned a total surface of 1439 ha. near Cardona, Barcelona province. The fire started at 2.44 p.m. local time, and it kept burning until 7.45 p.m. approximately, when the fire was considered stabilised by the firefighters because the perimeter remained stable, but it was not controlled until 8.30 p.m. on the following day.

The initial burnt area was covered mainly with *Pinus nigra* and *Pinus halepensis*, where the fire run with light southwesterly winds, generating a first fire perimeter of almost 3 km distance between the head and the back of the fire. The smoke column then turned to the north, and the rate of spread and the spotting distance increased. Fortunately, the fire reached the area affected by the 1994's fire with lower fuel loading, covered with pastoral land. This made it possible to contain the fire.

The registered wind speed range varied from 4.8 m/s to 2.2 m/s and the wind direction ranged from 183 degrees east of north to 190 degrees. This wind data do not explain the change in fire spread rate and direction, and it was therefore rose the hypothesis of the influence of the topography and the fire itself in the micro-meteorological conditions [2]. The burnt area was located at an altitude ranging from 332 metres to 748 metres above sea level, with areas of high slope.

In this example, the simulation area is bigger, a rectangle of $6.885\,m \times 6.575\,m$, and the simulation of each hour of fire spread involves about 7.30 minutes of computational time on the same laptop as the previous example. In this case, a total of 4 hours and a half have been simulated, updating wind data every half hour, with a total simulation time of 33 minutes. The average similarity indexes obtained in this case also show a good degree of similarity between actual and simulated perimeters: Sørensen similarity index $S = 0.81$, Jaccard similarity coefficient $J = 0.69$ and Kappa coefficient $K = 0.70$.

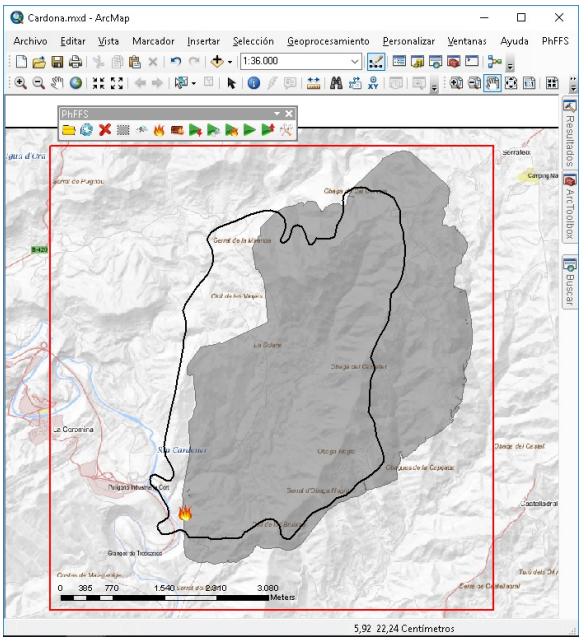

Figure 4: Comparison of the actual perimeter (black line) and simulated perimeter (grey area) after four hours and a half in Cardona fire, Barcelona, 8 July 2005.

5 Conclusions

This paper presents a GIS-based interface for two simplified physical models, a wildland fire spread model, PhFFS, and a wind field model, HDWF, which can work coupled or separately. The development of this tool has required interdisciplinary collaboration, including the participation of GIS ex-

perts, forest engineers and professionals with direct experience in wildfire fighting. Furthermore, it has been necessary a previous spatial data analysis and assembling for processing custom maps that enables an optimal use of the tool throughout Spain.

Technical aspects of the models integration in a GIS platform are based on the extent of the functionality of the commercial software ArcGIS Desktop, through the Python scripting language and Esri's ArcPy library. Several scripts have been developed to automate geographical data acquisition, spatial data pre-processing, models configuration, models running, and the visualization of the simulation results on a basemap.

The initial purpose of the integration of the fire and wind models on a GIS-based interface is to facilitate the testing, validation and adjustment process, by automating and simplifying the data acquisition process and the display of the solution.

The GIS-based tool also makes the PhFFS and HDWF models more readily accessible to the potential end-user by providing a simple, intuitive and easy-to-use tool that is more accessible to a broader audience that might not be familiar with these models.

The complete simulation of either one of the physical processes that the tool supports, wildfire spread or wind field, includes three steps: pre-processing the requested data, running the models, and post-processing the solution. The scripts developed reduce pre-processing and post-processing times and prevent input data errors. The numerical techniques that both PhFFS and HDWF use guarantee shorter-than-real-time computational times. Reducing the total computational time is critical for the practical application of these models.

Some direct applications of the PhFFS model are the design of risk mapping, reforestation policies, or fuelbreaks in prevention operations; the optimization of fire-fighting resources, risk prevention, the issue of warnings or evacuation planning in suppression operations, along with others such as prescribed burn planning.

Certain additional functionalities of the designed tool may have an interesting potential for practical applications. Secondary fire sources (spotting) can be simulated by adding new ignition points. Some suppression works, such as firebreaks, can be simulated through the "firebreaks tool" on the application toolbar, enabling the user to test different scenarios.

The HDWF has other specific applications, such as wind power forecasting on wind farms.

Acknowledgements

This work has been partially supported by the Department of Education of the regional government, *Junta of Castilla y León*, Grant contract: SA020U16 with the participation of FEDER, and by *University of Salamanca General Foundation*, TCUE grant. The authors are also grateful to Arsenio Morillo, forest engineer of *Xunta of Galicia* and coordinator of the fire-suppression operations during the Osoño fire for his extensive and detailed data about that fire; and to the company Tecnosylva S.L. and *Bombers de la Generalitat de Catalunya* (GRAF) for all the information provided about the Cardona fire.

References

[1] H.E. Anderson. Aids to determining fuel models for estimating fire behavior. General Technical Report INT-122, U.S. Department of Agriculture, Forest Service, Intermountain Forest and Range Experiment Station, 1982.

[2] T. Artés, A. Cardil, A. Cortés, T. Margalef, D. Molina, L. Pelegrín, and J. Ramírez. Forest fire propagation prediction based on overlapping dddas forecasts. *Procedia Computer Science*, 51:1623 – 1632, 2015.

[3] M.I. Asensio and L. Ferragut. On a wildland fire model with radiation. *International Journal for Numerical Methods in Engineering*, 54(1):137–157, 2002.

[4] M.I. Asensio, L. Ferragut, and J. Simon. Modelling of convective phenomena in forest fire. *RACSAM - Revista de la Real Academia de Ciencias Exactas, Físicas y Naturales. Serie A. Matemáticas*, 96(3):299–313, 2002.

[5] M.I. Asensio, L. Ferragut, and J. Simon. A convection model for fire spread simulation. *Applied Mathematics Letters*, 18(6):673–677, 2005. Special issue on the occasion of MEGA 2003.

[6] B. Chapman, G. Jost, and R. Van Der Pas. *Using OpenMP: Portable Shared Memory Parallel Programming*. Scientific and Engineering Computation. MIT Press, 2008.

[7] ESRI. What is arcpy?, 2016. Available from: https://desktop.arcgis.com/en/arcmap/10.3/analyze/arcpy/ what-is-arcpy-.htm.

[8] L. Ferragut, M.I. Asensio, J.M. Cascón, and D. Prieto. *Advances in Differential Equations and Applications*, chapter A Simplified Wildland Fire Model Applied to a Real Case, pages 155–167. Number 4 in SEMA SIMAI Springer Series. Springer International Publishing, Cham, 2014.

[9] L. Ferragut, M.I. Asensio, J.M. Cascón, and D. Prieto. A wildland fire physical model well suited to data assimilation. *Pure and Applied Geophysics*, 172(1):121–139, 2015.

[10] L. Ferragut, M.I. Asensio, and S. Monedero. Modelling radiation and moisture content in fire spread. *Communications in Numerical Methods in Engineering*, 23(9):819–833, 2007.

[11] L. Ferragut, M.I. Asensio, and S. Monedero. A numerical method for solving convection-reaction-diffusion multivalued equations in fire spread modelling. *Advances in Engineering Software*, 38(6):366–371, 2007.

[12] L. Ferragut, M.I. Asensio, and J. Simon. High definition local adjustment model of 3d wind fields performing only 2d computations. *International Journal for Numerical Methods in Biomedical Engineering*, 27(4):510–523, 2011.

[13] L. Ferragut, R. Montenegro, G. Montero, E. Rodríguez, M.I. Asensio, and J.M. Escobar. Comparison between 2.5-d and 3-d realistic models for wind field adjustment. *Journal of Wind Engineering and Industrial Aerodynamics*, 98(10–11):548–558, 2010.

[14] J.B. Filippi, V. Mallet, and B. Nader. Representation and evaluation of wildfire propagation simulations. *International Journal of Wildland Fire*, 23:46–57, 2014.

[15] M. D. Flannigan, M. A. Krawchuk, W. J. de Groot, B. M. Wotton, and L. M. Gowman. Implications of changing climate for global wildland fire. *International Journal of Wildland Fire*, 18(5):483–507, 2009.

[16] IGN. Spanish land cover information system, 2011. Available from: http://www.ign.es/ign/layoutIn/siose.do.

[17] IGN. Modelo digital de elevación, 2012. Available from: http://centrodedescargas.cnig.es/CentroDescargas/index.jsp.

[18] R. Linn, J. Winterkamp, C. Edminster, J. J. Colman, and W. S. Smith. Coupled influences of topography and wind on wildland fire behaviour. *International Journal of Wildland Fire*, 16(2):183–195, 2007.

[19] Magrama. Spanish forestry map 1:50.000, January 2007. Available from: http://www.magrama.gob.es/es/biodiversidad/servicios/banco-datos-naturaleza/informacion-disponible/mfe50.aspx.

[20] Magrama. Third spanish national forest inventory, 2007. Available from: http://www.magrama.gob.es/es/biodiversidad/servicios/banco-datos-naturaleza/informacion-disponible/ifn3.aspx.

[21] Magrama. Fourth spanish national forest inventory, 2016. Available from: http://www.magrama.gob.es/es/desarrollo-rural/temas/politica-forestal/inventario-cartografia/inventario-forestal-nacional/.

[22] Magrama. National topographic base 1:25.000, 2016. Available from: http://centrodedescargas.cnig.es/CentroDescargas/index.jsp.

[23] Magrama. Spanish forestry map 1:25.000, 2016. Available from: http://www.mapama.gob.es/es/desarrollo-rural/temas/politica-forestal/inventario-cartografia/mapa-forestal-espana/mfe_25.aspx.

[24] D. Prieto, M.I. Asensio, L. Ferragut, and J.M. Cascón. Sensitivity analysis and parameter adjustment in a simplified physical wildland fire model. *Advances in Engineering Software*, 90:98–106, 2015.

[25] G. Schmuck, J. San-Miguel-Ayanz, T. Durrant, R. Boca, G. Libertá, T. Petroliagkis, M. Di Leo, D. Rodrigues, F. Boccacci, and E. Schulte. Forest fires in europe, middle east and north africa 2014. Technical report EUR 27400 EN, Institute for Environment and Sustainability. Joint Research Centre. European Commission, Luxembourg, 2015. Available from: http://forest.jrc.ec.europa.eu/effis/reports/annual-fire-reports.

[26] D.X. Viegas. Slope and wind effects on fire propagation. *International Journal of Wildland Fire*, 13(2):143–156, 2004.